

Figure S1. Purification of *E. coli* σ^{32} -Rpo complex and Cryo-EM of the *E. coli* σ^{32} -Rpo complex. (A) Chromatogram map of gel filtration. (B) SDS-PAGE of the purified complex. (C) Pipeline of the cryo-EM data processing. (D) The Fourier shell correlation (FSC) analysis. The dotted line represents the 0.143 FSC cut off. The final resolution is determined at 2.49 Å. (E) The angular distributions of *E. coli* σ^{32} -Rpo particle and Density map for *E. coli* σ^{32} -Rpo, colored by local resolution.



Figure S2. Sequence alignment of σ factors. Sequence alignment analysis between σ^{32} , σ^{70} , σ^{38} , σ^{28} . The experimentally validated residues in σ_4 , σ_3 , and σ_2 are indicated with red, purple and blue stars, respectively. The promoter unwinding residues in σ_2 are shown in light blue frame. The replaced region in the σ_4 tail of σ^{38} , σ^{28} is shown in light brown frame, consistent with diagrams in Figure 3E.

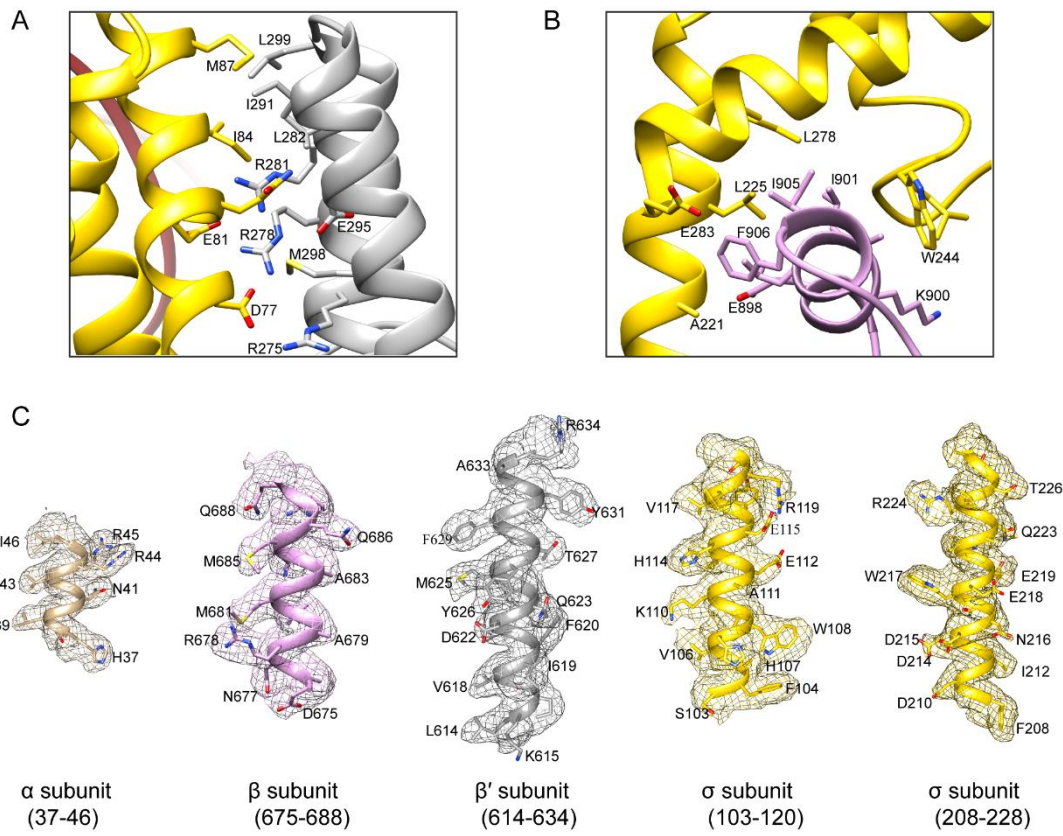


Figure S3. Structural and interacted details of pointed motifs. (A) The interaction details between σ_2 and β' clamp helix. (B) The interaction details between σ_4 and β FTH. (C) The structural details in α , β , β' , and σ^{32} motifs.

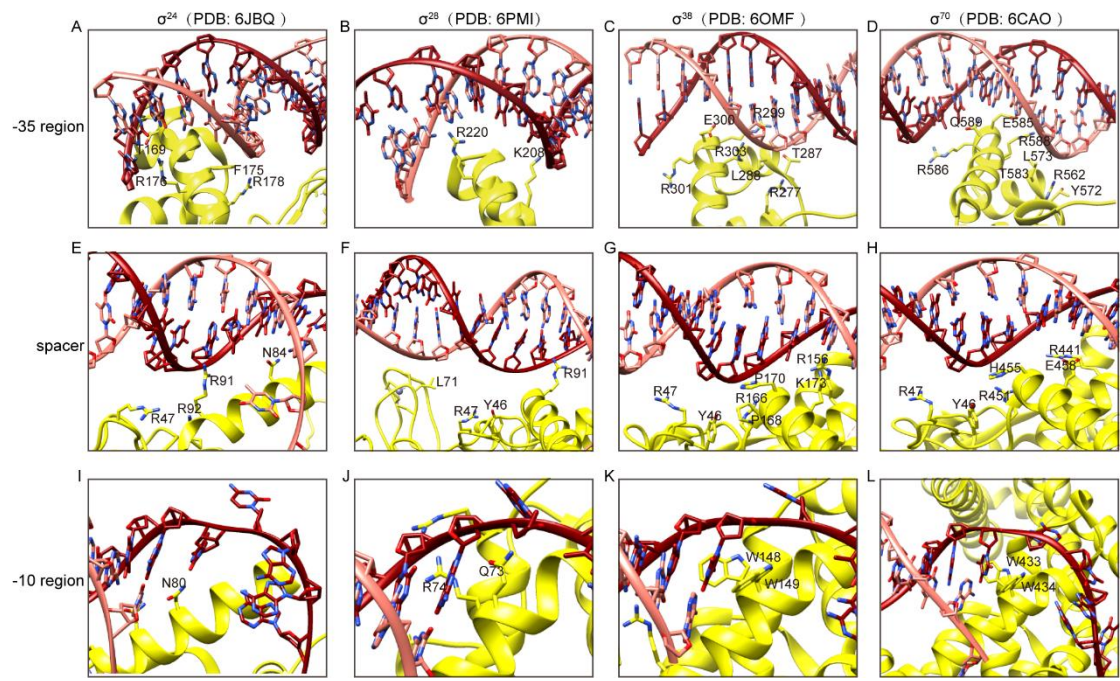


Figure S4. The detailed interactions between σ s (σ^{24} , σ^{28} , σ^{38} and σ^{70}) and corresponding promoters. (A-D) The interaction details between σ_4 (σ^{24} , σ^{28} , σ^{38} and σ^{70}) and corresponding -35 elements. (E-H) The interaction details between σ_3 (σ^{24} , σ^{28} , σ^{38} and σ^{70}) and corresponding spacer regions. (I-L) The wedge residues in different σ s (σ^{24} , σ^{28} , σ^{38} and σ^{70}).

Table S1. Kinetic parameters from Figure. 2C of RPo formation by *E. coli* RNAP holoenzyme comprising wild-type or derivatives of *E. coli* σ^{32} .

Samples	a_1	$k_{obs,1} (\text{s}^{-1})$	a_2	$k_{obs,2} (\text{s}^{-1})$
<i>Ec</i> holo σ^{32} (WT)	1.719 \pm 0.008	0.1102 \pm 0.0007	2.819 \pm 0.003	0.0107 \pm 0.0004
<i>Ec</i> holo σ^{32} (V97A)	1.532 \pm 0.006	0.0362 \pm 0.0009	2.596 \pm 0.003	0.0069 \pm 0.0003
<i>Ec</i> holo σ^{32} (N94A)	1.446 \pm 0.007	0.0911 \pm 0.0005	2.361 \pm 0.002	0.0104 \pm 0.0006
<i>Ec</i> holo σ^{32} (H107A)	1.179 \pm 0.006	0.0242 \pm 0.0015	2.426 \pm 0.002	0.0063 \pm 0.0005
<i>Ec</i> holo σ^{32} (F104A)	0.969 \pm 0.005	0.0244 \pm 0.0018	2.077 \pm 0.002	0.0061 \pm 0.0002
<i>Ec</i> holo σ^{32} (W108A)	0.895 \pm 0.004	0.0599 \pm 0.0011	1.556 \pm 0.001	0.0079 \pm 0.0002
<i>Ec</i> core	0.155 \pm 0.058	0.0136 \pm 0.0038	0.289 \pm 0.001	0.0047 \pm 0.0003

Table S2. Kinetic parameters from Figure. 2D of RPo formation by *E. coli* RNAP holoenzyme comprising wild-type or derivatives of *E. coli* σ^{32} .

Samples	a_1	$k_{obs,1} (\text{s}^{-1})$	a_2	$k_{obs,2} (\text{s}^{-1})$
<i>Ec</i> holo σ^{32} (WT)	1.770 \pm 0.010	0.1199 \pm 0.0033	2.773 \pm 0.003	0.0144 \pm 0.0007
<i>Ec</i> holo σ^{32} (WW)	1.819 \pm 0.009	0.1424 \pm 0.0022	3.019 \pm 0.003	0.0122 \pm 0.0006
<i>Ec</i> holo σ^{32} (QR)	1.122 \pm 0.006	0.0899 \pm 0.0006	1.675 \pm 0.002	0.0079 \pm 0.0005
<i>Ec</i> core	0.156 \pm 0.002	0.0148 \pm 0.0002	0.289 \pm 0.001	0.0015 \pm 0.0003

RNAP holoenzyme comprising wild-type or derivatives of *E. coli* σ^{32} .